AIP Journal of Applied Physics

# Temperature dependent electrical transport studies of self-aligned ZnO nanorods/Si heterostructures deposited by sputtering

Sapana Ranwa, Pawan Kumar Kulriya, Vivek Dixit, and Mahesh Kumar

Citation: Journal of Applied Physics **115**, 233706 (2014); doi: 10.1063/1.4883961
View online: http://dx.doi.org/10.1063/1.4883961
View Table of Contents: http://scitation.aip.org/content/aip/journal/jap/115/23?ver=pdfcov
Published by the AIP Publishing

**Articles you may be interested in**

Double Gaussian distribution of barrier height observed in densely packed GaN nanorods over Si (111) heterostructures
J. Appl. Phys. **116**, 234508 (2014); 10.1063/1.4904749

Tuning the emission of ZnO nanorods based light emitting diodes using Ag doping
J. Appl. Phys. **116**, 193104 (2014); 10.1063/1.4902526

High quality boron carbon nitride/ZnO-nanorods p-n heterojunctions based on magnetron sputtered boron carbon nitride films
Appl. Phys. Lett. **105**, 192104 (2014); 10.1063/1.4901273

Studies on ZnO nanorods/ CuInS 2 coaxial n-p heterojunction arrays
AIP Conf. Proc. **1512**, 1024 (2013); 10.1063/1.4791392

High sensitivity and fast response and recovery times in a ZnO nanorod array/p-Si self-powered ultraviolet detector
Appl. Phys. Lett. **101**, 261108 (2012); 10.1063/1.4773245

[This article is copyrighted as indicated in the article. Reuse of AIP content is subject to the terms at: http://scitation.aip.org/termsconditions. Downloaded to ] IP: 136.165.238.131 On: Wed, 24 Dec 2014 00:28:00

JOURNAL OF APPLIED PHYSICS 115, 233706 (2014)

# Temperature dependent electrical transport studies of self-aligned ZnO nanorods/Si heterostructures deposited by sputtering

Sapana Ranwa,[1] Pawan Kumar Kulriya,[2] Vivek Dixit,[1] and Mahesh Kumar[1,a)]
[1]Centre for Information and Communication Technology, Indian Institute of Technology Jodhpur, Jodhpur 342011, India
[2]Inter University Accelerator Centre, Aruna Asaf Ali Marg, New Delhi 110067, India

(Received 12 May 2014; accepted 5 June 2014; published online 17 June 2014)

Self-aligned ZnO nanorods (NRs) were grown on n-Si(100) substrate by RF sputtering techniques. The NRs are uniformly grown on 2-inch wafer along [0001] direction. Single-crystalline wurtzite structure of ZnO NRs was confirmed by X-ray diffraction. The average diameter, height, and density of NRs are found 48 nm, 750 nm, and $1.26 \times 10^{10}$ cm$^{-2}$, respectively. The current-voltages (*I-V*) characteristics of ZnO NRs/Si heterojunction (HJ) were studied in the temperature range of 120–300 K and it shows a rectifying behavior. Barrier height ($\phi_B$) and ideality factor ($\eta$) were estimated from thermionic emission model and found to be highly temperature dependent in nature. Richardson constant ($A^*$) was evaluated using Richardson plot of $\ln(I_o/T^2)$ versus q/kT plot by linear fitting in two temperature range 120–180 K and 210–300 K. Large deviation in Richardson constant from its theoretical value of n-Si indicates the presence of barrier inhomogeneities at HJ. Double Gaussian distribution of barrier height with thermionic equation gives mean barrier heights of $0.55 \pm 0.01$ eV and $0.86 \pm 0.02$ eV for two different temperature regions 120–180 K and 210–300 K, respectively. Modified Richardson plot provided two values of Richardson constant for two temperature regions. However, for higher temperature range (210–300 K), the calculated value of Richardson constant ~123 A cm$^{-2}$ K$^{-2}$ was close to the ideal Richardson constant for n-Si. © *2014 AIP Publishing LLC*. [http://dx.doi.org/10.1063/1.4883961]

## I. INTRODUCTION

ZnO with large band-gap (~3.3 eV) and large excitation binding energy (~60 meV), enchant many researchers interest due to its remarkable performance in electronic and photonic devices.[1] In recent years, nanostructure materials have attracted much attention due to their unique electronic, optoelectronic, piezoelectric, and mechanical properties. The performances of such nanodevices are expected to be superior as the quantum confinement of charge carriers in small dimension gives rise to spectacular variation in properties.[2,3] ZnO nanostructures of various types such as nanowires (NWs), nanotubes (NTs), and nanorods (NRs) have been widely studied due to their unique material properties and used in various applications such as gas sensors,[4] UV lasers,[5] solar cells,[6] photodetectors, bio-sensors,[7] and light emitted diode.[8] Due to the presence of native defects, zinc interstitial vacancies, ZnO always behaves as n type semiconductor.[9] ZnO NRs or thin film based heterojunction (HJ) were grown upon various substrate such as Si,[10–12] sapphire,[13] and ITO.[14] The junction between two materials plays an important role in semiconductor devices and affecting the performance of the device. Normally, temperature dependent current-voltage (*I-V-T*) characteristic is used to explain the conduction mechanism and barrier inhomogeneities at ZnO/Si HJ. Thermionic emission (TE) is always predominating carrier transport mechanism to extract barrier height ($\phi_B$) and ideality factor ($\eta$) at heterojunction in forward bias current voltage (*I-V*) characteristics. However, experimental temperature dependent *I-V* data for various ZnO based heterostructure shows rectifying behavior in forward bias.[15] At low temperature, majority carriers (electrons) do not get sufficient energy to cross barrier and electrons start tunneling through defects and lower the barrier heights. As temperature increases, electrons gain sufficient energy to overcome higher barrier thus with temperature barrier height increases and ideality factor decreases.[16,17] The nonlinearity due to barrier inhomogeneities and defects at heterojunction is determined from the activation plot $\ln(I_0/T^2)$ versus q/kT.[18,19] Gaussian distribution of barrier height with thermionic emission theory is one of the effective method to explain temperature dependence of barrier height. The mean barrier height and Richardson constant calculated using Gaussian distribution to thermionic emission are found to be close to theoretical values.[16] Yilmaz *et al.*[20] analyzed ZnO/n-ZnO NR HJ by using standard TE theory with the assumption of a Gaussian distribution of the barrier heights. In case of n-ZnO NWs/p-Si HJ diode, higher value of Richardson constant is observed due to the presence of barrier inhomogeneity phenomenon.[21] In the present paper, effect of the temperature on the electrical transport behavior of RF sputtering grown ZnO NRs/Si HJ is studied. The experimental results are explained on the basis of the TE model with Gaussian distributions.

## II. EXPERIMENTAL PROCEDURE

ZnO NRs were deposited on 2-inch-Si wafers by RF magnetron sputtering technique. The n-Si(100) substrates

a)Author to whom correspondence should be addressed. Electronic mail: mkumar@iitj.ac.in

 © 2014 AIP Publishing LLC

[This article is copyrighted as indicated in the article. Reuse of AIP content is subject to the terms at: http://scitation.aip.org/termsconditions. Downloaded to ] IP: 136.165.238.131 On: Wed, 24 Dec 2014 00:28:00

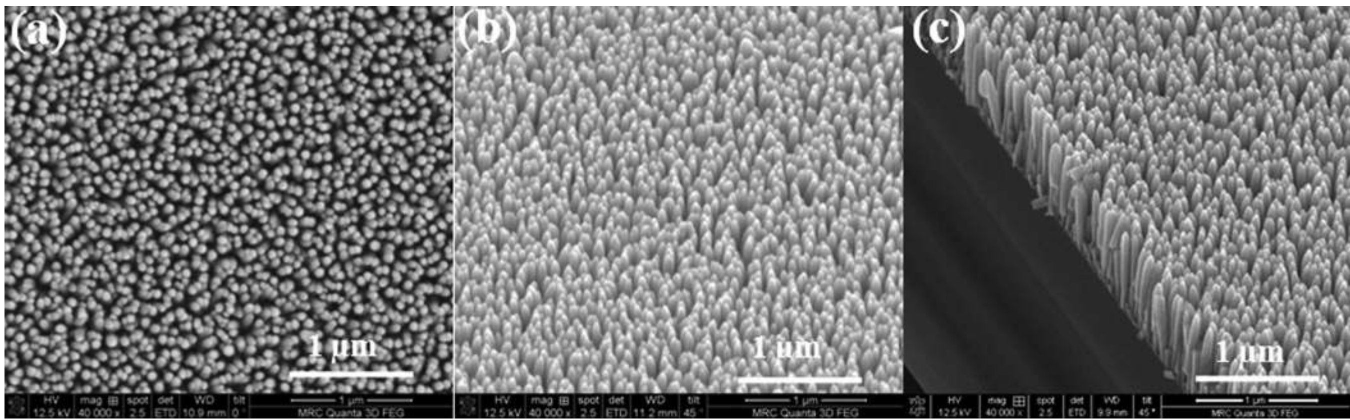


FIG. 1. FESEM images of ZnO NRs (a) top view, (b) 45° tilted, and (c) cross-sectional view.

(resistivity ~0.01–0.02 Ω cm) were chemically cleaned followed by dipping in 5% HF to remove the surface oxide. ZnO target with purity (99.999%) were used as source materials and base pressure of vacuum chamber was maintained up to $1 \times 10^{-6}$ mbar. The deposition was carried out in the presence of pure Ar gas (99.999%) and chamber pressure was maintained $2 \times 10^{-2}$ mbar during deposition. Substrate temperature, target to substrate distance, RF power, and Ar flow rate were kept at 500 °C, 14 cm, 150 W, and 60 sccm, respectively. The duration of NRs deposition was 2 h. Structural and optical characterization of ZnO nanorods was carried out using X-Ray diffraction (XRD) and Raman spectroscopy. Surface morphologies were carried out using Atomic Force Microscopy (AFM) and field emission scanning electron microscopy (FE-SEM). Optical band-gap of ZnO NRs was measured by diffused UV-Vis spectroscopy. The aluminium (Al) circular contacts of diameter 500 $\mu$m were fabricated on ZnO NRs and on n-Si by thermal evaporation using a physical mask. Temperature dependent *I-V* characterizations of the device were carried out on probe station with Keithley-2612 system source meter.

## III. RESULTS AND DISCUSSION

Figs. 1(a)–1(c) show typical FE-SEM images of top view, 45° tilted, and cross-sectional view of ZnO NRs, respectively. It can be seen in the figure that the as-grown NRs are vertically aligned and uniformly grown over the entire substrate. The average length, diameter, and density of rods are found to be approximately 750 nm, 48 nm, and $1.26 \times 10^{10}$ cm$^{-2}$, respectively. Figs. 2(a) and 2(b) show the 2-D and 3-D view AFM images of the ZnO NRs, which indicates that NRs are uniformly distributed throughout the substrate with average diameter of ~48 nm. The structural characterization of ZnO NRs was evaluated by XRD and shown in Fig. 3(a). The appearance of the single peak at 34.64° in the $2\theta$-$\omega$ scan indicating that ZnO NRs are highly c-oriented along [0001] direction of hexagonal wurtzite structure. The full width half maxima (FWHM) of (0002) peak is 12 arcmin, which is consistence with earlier reported value of the ZnO.[22]

The optical band gap of ZnO NRs was measured by diffused reflectance spectroscopy over UV-Vis spectroscopy and shown in Fig. 3(b). Diffused reflectance spectra were converted into Kubelka-Munk transformed reflectance spectra to calculate band gap of ZnO NRs.[23] The band gap of ZnO NRs was calculated by extrapolating the linear region of $(K \times h\nu)^2$ versus $h\nu$ graph and found to be ~3.24 eV which is close to the literature values.[23] The crystalline quality and lattice structures of ZnO NRs were further investigated by micro-Raman spectroscopy and shown in Fig. 3(c). Micro-Raman measurement was analyzed using back scattering geometry from spectra physics with the help of 50 mW argon ion laser that is corresponding to 514.5 nm phonon excitation. According to Senthil *et al.*,[24] there are only two Raman active vibration modes $E_2$(high) and $A_1$(LO) are allowed for the c-axies ZnO NWs. From the figure, it can be seen that except the substrate peaks, a strong, peak is

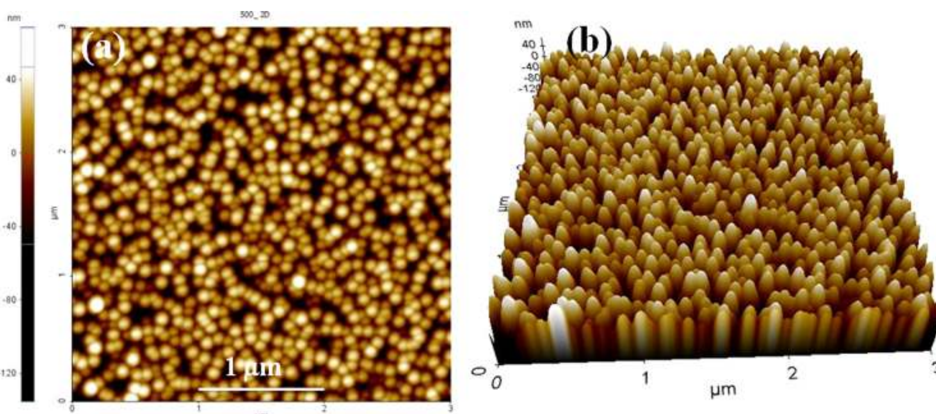


FIG. 2. AFM images of ZnO NRs (a) 2-D view and (b) 3-D view.

[This article is copyrighted as indicated in the article. Reuse of AIP content is subject to the terms at: http://scitation.aip.org/termsconditions. Downloaded to ] IP: 136.165.238.131 On: Wed, 24 Dec 2014 00:28:00

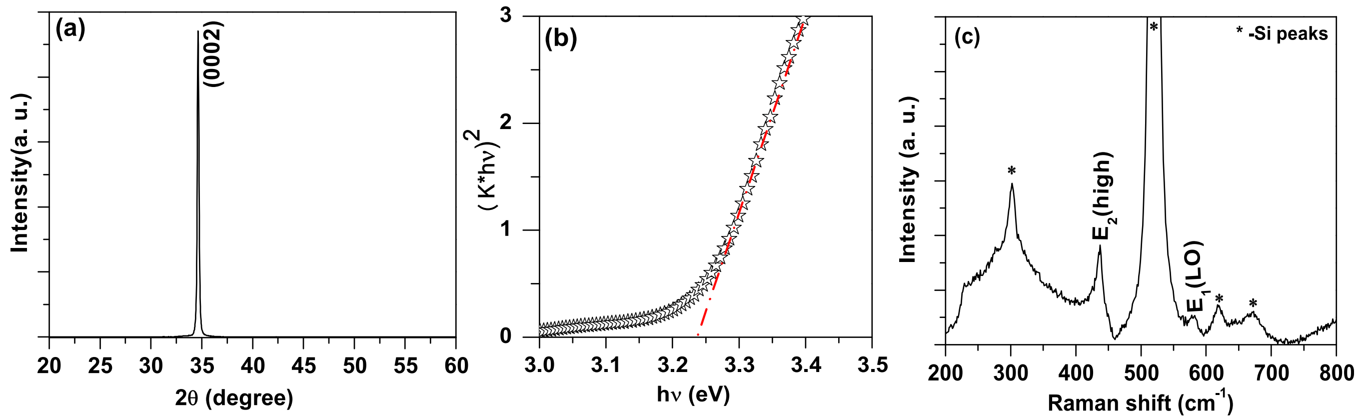


FIG. 3. (a) XRD 2$\theta$-$\omega$ scan, (b) variation of $(K \times h\nu)^2$ with photon energy ($h\nu$), and (c) Raman scattering spectra of ZnO NRs deposited on n-Si(100) substrate.

appearing at 438 $cm^{-1}$ that attributes to $E_2$ (high) mode. This indicates that ZnO NRs are crystalline and having hexagonal wurtzite structure. It may also be noted that there is a weak peak appearing at 582 $cm^{-1}$, is corresponding to $E_1$(LO) mode. The appearance of this peak confirms the presence of oxygen vacancy and zinc interstitials, such type of the defects are commonly observed in the undoped ZnO.[25,26]

The schematic diagram of the device is shown in Fig. 4(a). The ohmic nature of Al contacts on Si and on ZnO was confirmed by *I-V* measurements and shown in Fig. 4(b). Fig. 5(a) shows room temperature *I-V* characterization of n-ZnO NRs/n-Si heterostructure and the *I-V* characteristic shows rectifying behavior which reveals formation of Schottky barrier at ZnO NRs/n-Si HJ. The current rectification ratio was calculated to be 3.6 at 2.5 V and leakage current is 3.5 mA. The smaller rectification ratio and large leakage current behavior can be explained by Electron Affinity Model (EAM). Due to smaller value of conduction band offset than valance band offset, electrons flow as majority carrier from Si to ZnO at HJ. Conduction band and valance band offsets are calculated by using EAM model, $\Delta E_C = \chi_{ZnO} - \chi_{Si}$ and $\Delta E_V = E_{g,ZnO} - E_{g,Si} + \Delta E_C$ (where $\chi_{ZnO} = 4.35$, $\chi_{Si} = 4.05$, $E_{g,ZnO} = 3.24$ eV, $E_{g,Si} = 1.12$ eV). The value of conduction and valence band offsets are found to be $\sim$0.3 eV and $\sim$2.42 eV, respectively. As temperature increases, forward bias current increases with decrease in turn on voltage. Fig. 5(b) shows the current conduction mechanism of ZnO NRs/n-Si HJ in forward bias condition at room temperature. From the figure, three distinct regions (I, II, and III) can be seen, which depend on the applied voltage. For region I ($V \leq 0.6$ V), current obeys Ohmic law, in which current increases linearly with voltage ($I \sim V$) due to thermally generated carrier tunneling. For region II ($0.6 < V \leq 1.65$ V), current exponentially increases with voltage ($I \propto \exp(\alpha V)$). This mechanism usually observed in wide bandgap semiconductor heterojunction diode due to recombination tunneling mechanism.[27] The $\alpha = 1.69\ V^{-1}$ was calculated by using exponential fitting in this region. For region III ($1.65 < V \leq 2.5$ V), current increases with voltage and satisfies power law ($I \propto V^n$) where n = 3.3. In this region, current follows space charge limited conduction mechanism in which current conduction through heterojunction is due to single charge carriers (electrons). Forward bias *I-V* characteristics of ZnO NRs/n-Si heterostructure were measured at different temperatures in the temperature range of 120–300 K and shown in Fig. 5(c). Thermionic emission model used to calculate Schottky barrier height ($\phi_B$) and ideality factor (η) for the ZnO NRs/Si HJ by fitting linear region of forward bias *I-V* characteristics. The *I-V* characteristics of n-ZnO NRs/n-Si HJ is given by[28,29]

$$I = I_o\left\{\exp\left(\frac{qV}{\eta kT}\right) - 1\right\}, \tag{1}$$

where $\eta$ is the ideality factor and $I_o$ is reverse saturation current given by following relation:

$$I_o = AA^*T^2 \exp\left(\frac{-q\phi_B}{kT}\right). \tag{2}$$

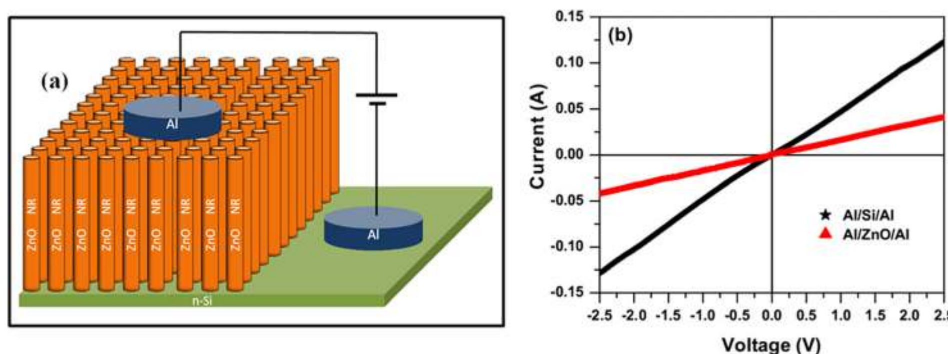


FIG. 4. (a) schematic of the device structure and (b) I-V characteristics of Al/Si/Al and Al/ZnO/Al contacts.

[This article is copyrighted as indicated in the article. Reuse of AIP content is subject to the terms at: http://scitation.aip.org/termsconditions. Downloaded to ] IP: 136.165.238.131 On: Wed, 24 Dec 2014 00:28:00

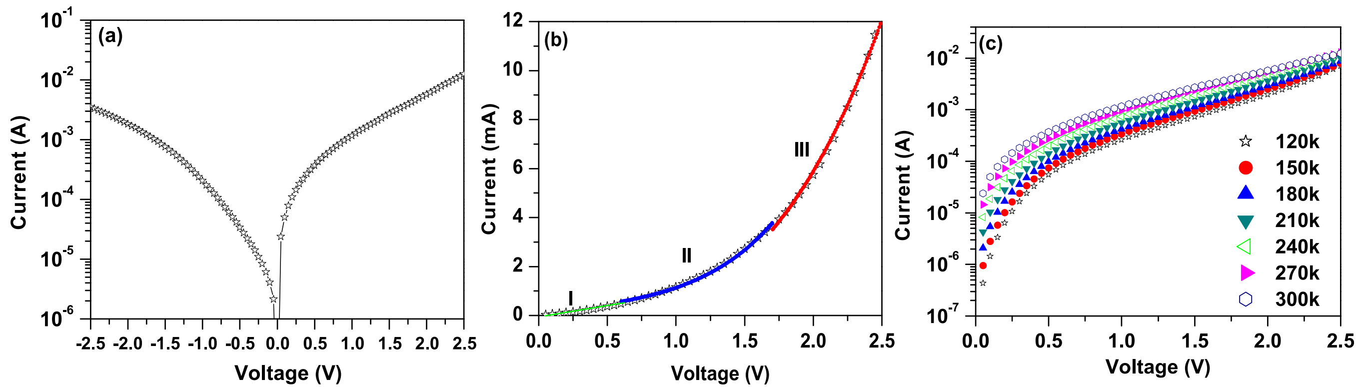


FIG. 5. (a) Room temperature I-V characteristics of ZnO NRs/Si HJ, (b) current conduction mechanism, and (c) forward bias temperature dependent I-V characteristics in temperature range 120–300 K.

Here $A^*$ is Richardson's constant (∼112 A $cm^{-2}$ $K^{-2}$ for n-Si), $A$ is contact area, $q$ is electron charge, T is measurement temperature in Kelvin, k is Boltzmann constant, and $\phi_B$ is effective Schottky barrier height. The ideality factor ($\eta$) and effective barrier height ($\phi_B$) were calculated by fitting linear region of the forward bias in Eq. (1). Fig. 6 shows barrier height and ideality factor varies with temperature and it can be seen from figure that barrier height increases and ideality factor decreases with temperature in temperature range 120–300 K. The barrier height and ideality factor vary from 0.24 eV to 0.54 eV and 5.5 to 3.5, respectively, for temperature from 120 to 300 K. Because of inhomogeneities and presence of defects at HJ, barrier height shows temperature dependent behavior.[20,21] Chirakkara and Krupanidhi[16] reported that the barrier height for n-ZnO/p-Si HJ varies from 0.60 eV to 0.76 eV as temperature increased from 300 to 390 K. At low temperature, the electrons are able to surmount the lower barriers and current transport is dominated by current flowing through the defects or intermediate states at ZnO NRs/Si interface. As the temperature increases, the more electrons have sufficient energy to surmount the higher barrier and as a result, the dominant barrier height increases with temperature.[30]

Non-ideal behavior of n-ZnO NRs/n-Si HJ diode can be explained by Richardson plot ($\ln(I_o/T^2)$ versus q/kT) using rearrangement of reverse saturation current equation

$$\ln\left(\frac{Io}{T^2}\right) = \ln(AA^*) - \frac{q\phi_B}{kT}. \tag{3}$$

By linear fitting of Richardson plot for different temperature ranges, it gives Richardson constant and barrier height. Fig. 7 shows temperature dependent $\ln(I_o/T^2)$ versus q/kT plot for 120–300 K temperature region. Richardson plot gives two linear regions for two different temperature ranges 120–180 K and 210–300 K. The calculated values of Richardson constant ($A^*$) and barrier height ($\phi_B$) for first region (120–180 K) are $1.02 \times 10^{-7}$ A $cm^{-2}$ $K^{-2}$ and 0.028 eV, whereas corresponding value for the second region (210–300 K) are $1.20 \times 10^{-6}$ A $cm^{-2}$ $K^{-2}$ and 0.067 eV. Larger changes in the Richardson constants indicate the presence of barrier inhomogeneities at HJ, which results in large deviation in barrier height for both temperature ranges. Tung[19] reported Gaussian distribution of barrier height using thermionic equation with mean barrier height ($\overline{\phi_B}$) and standard deviation ($\sigma$) of barrier height. Small value of standard deviation is observed for less barrier inhomogeneities at junction. Gaussian distribution of barrier height can be given as[31]

$$P(\phi_B) = \frac{1}{\sigma\sqrt{2\pi}} \exp\left[-\frac{(\phi_B - \overline{\phi_B})}{2\sigma^2}\right], \tag{4}$$

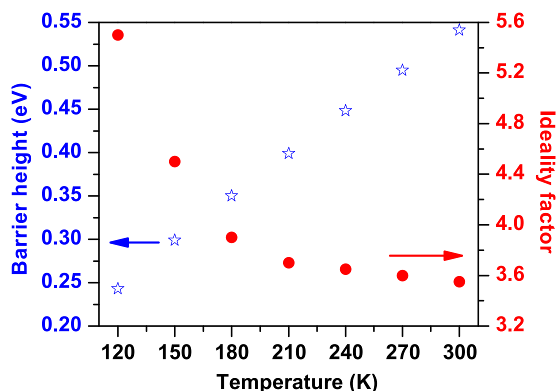


FIG. 6. Temperature dependent variation of ideality factor and barrier height of ZnO NRs/Si HJ.

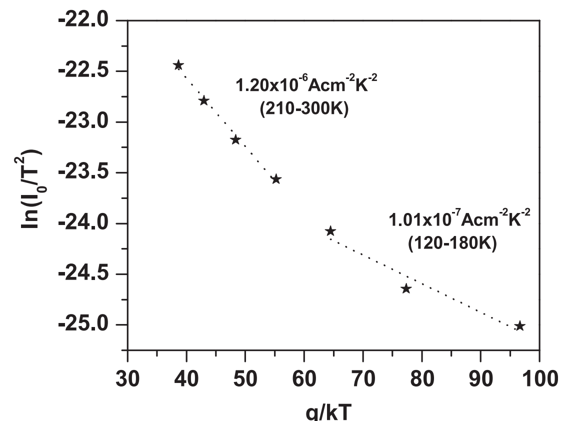


FIG. 7. Richardson plot of $\ln(I_o/T^2)$ versus q/kT.

[This article is copyrighted as indicated in the article. Reuse of AIP content is subject to the terms at: http://scitation.aip.org/termsconditions. Downloaded to ] IP: 136.165.238.131 On: Wed, 24 Dec 2014 00:28:00

where the effective barrier height can be represented as a function of q/2kT, given as

$$\phi_B = \overline{\phi_B} - \frac{q\sigma^2}{2kT}. \quad (5)$$

Fig. 8 shows effective barrier height versus q/2kT plot as function of temperature. By using linear fitting, intercept point of straight line at zero gives mean barrier height ($\overline{\phi_B}$) and slop of line gives standard deviation ($\sigma^2$). Observation of two different linear regions (temperature range 120–180 K and 210–300 K) indicates double Gaussian distribution of barrier height at n-ZnO NRs/n-Si HJ.[32] For these two Gaussian region, calculated value of mean barrier height and standard deviation ($\sigma^2$) are $0.55 \pm 0.01$ eV and 0.0065 (120–180 K for region I) and $0.86 \pm 0.02$ eV and 0.017 (210–300 K for region II), respectively. At low temperatures, electron does not have enough energy to surmount the barrier and it will tunnel through the defects at the interface. Hence, at low temperature (120–180 K), the current is dominated by field effect (FE) mechanism as tunneling-dominated current transport.[32] At higher temperature (210–300 K), the carriers have enough energy to surmount the barrier and current transport is dominated by TE mechanism.

For the calculation of Richardson constant, Gaussian distribution applied to the Richardson constant equation that gives modified Richardson constant equation as stated below

$$\ln\left(\frac{Io}{T^2}\right) - \left(\frac{q^2\sigma^2}{2k^2T^2}\right) = \ln(AA^*) - \frac{q\overline{\phi_B}}{kT}. \quad (6)$$

Fig. 9 shows modified Richardson plot of $\ln\left(\frac{Io}{T^2}\right) - \left(\frac{q^2\sigma^2}{2k^2T^2}\right)$ versus q/2kT. Mean barrier height and Richardson constant were calculated from the slop and intercept of the linear fitted curve. Richardson constants and mean barrier heights are 136.3 A $cm^{-2}$ $K^{-2}$ and 0.55 eV for region I (120–180 K) and 123.4 A $cm^{-2}$ $K^{-2}$ and 0.86 eV for region II (210–300 K), respectively. Mean barrier height value has resemblance to mean barrier height obtain from Gaussian distribution of barrier height plot. At higher temperature range (210–300 K), Richardson constant value is more close to theoretical value of Richardson constant of n-Si (112 A $cm^{-2}$ $K^{-2}$) than lower temperature region (120–180 K). Somvanshi and Jit[21] also

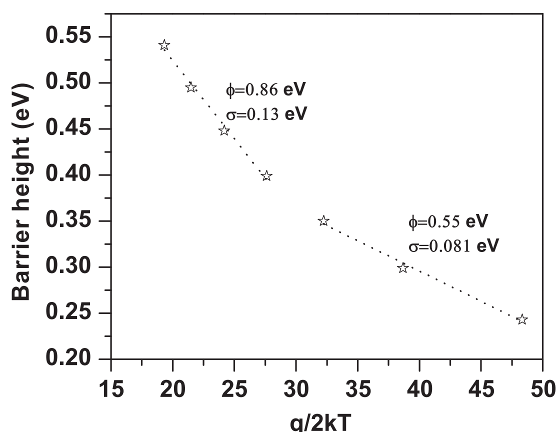


FIG. 8. Plot of effective barrier height versus q/kT.

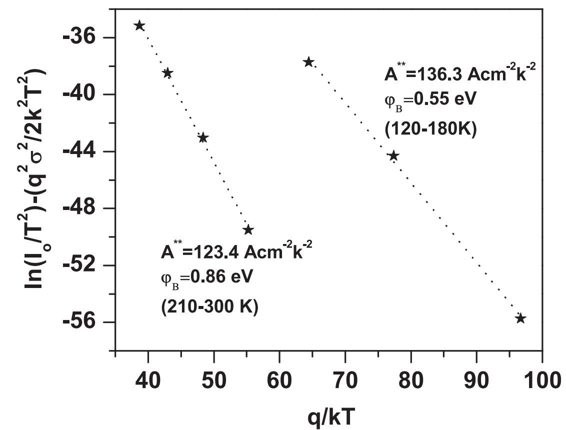


FIG. 9. Modified Richardson plot of $\ln\left(\frac{Io}{T^2}\right) - \left(\frac{q^2\sigma^2}{2k^2T^2}\right)$ versus q/2kT.

reported the deviated of Richardson constant from 32 A $cm^{-2}$ $K^{-2}$ to 49 A $cm^{-2}$ $K^{-2}$ for n-ZnO. Consideration of barrier inhomogeneities distribution at junction gives more appropriate value of Richardson constant. Quemener *et al.*[28] fabricated HJ by atomic layer deposition and the barrier heights to be found 0.61 eV and 0.52 eV for n-ZnO/n-Si HJ and n-ZnO /p-Si HJ, respectively, for temperature range 180–280 K. In the present study, the barrier height extracted using Gaussian distribution and modified Richardson plot for higher temperature range (210–300 K) gives mean barrier height 0.86 eV which is slightly higher than earlier reported value.[29] The higher barrier height value could be due to the presence of a thin oxide layer ($<$3 nm) between ZnO and Si, which is commonly found in RF sputtered HJs.

## IV. CONCLUSION

ZnO NRs were uniformly grown of 2-inch Si wafer by RF sputtering. The average diameter, height, and density of NRs are measured from FE-SEM and found to be 48 nm, 750 nm, and $1.26 \times 10^{10}$ $cm^{-2}$, respectively. XRD $2\theta$-$\omega$ scan revealed that NRs are highly c-oriented along [0001]. Electrical *I-V* characterization of ZnO NRs/Si HJ was investigated in the range of 120–300 K. Ideality factor and barrier height of the HJ were estimated from TE and found to be highly temperature dependent in nature due to the presence of defects and barrier inhomogeneities at junction. Linear fitting of $\ln(I_o/T^2)$ versus q/kT plot gives two different Richardson constant values in 120–180 K and 210–300 K ranges. Large deviation in Richardson constant indicates the presence of barrier inhomogeneities at junction. Double Gaussian distribution of barrier height with thermionic emission gives mean barrier heights 0.55 eV and 0.86 eV for two different temperature regions 120–180 K and 210–300 K, respectively. Modified Richardson constant $\sim$123 A $cm^{-2}$ $K^{-2}$ in the temperature range of 210–300 K is close to theoretical value of n-Si, indicating that the TE model with a Gaussian distribution of barrier heights could explain the experimental data.

[1] U. Ozgur, Y. I. Alivov, C. Liu, A. Teke, M. A. Reshchikov, S. Dogan, V. Avrutin, S. J. Cho, and H. Morkoc, J. Appl. Phys. **98**, 041301 (2005).
[2] K. F. Lin, H. M. Cheng, H. C. Hsu, and W. F. Hsieh, Appl. Phys. Lett. **88**, 263117 (2006).

[This article is copyrighted as indicated in the article. Reuse of AIP content is subject to the terms at: http://scitation.aip.org/termsconditions. Downloaded to ] IP: 136.165.238.131 On: Wed, 24 Dec 2014 00:28:00

[3]Y. Gu, I. L. Kuskovsky, M. Yin, S. O'Brien, and G. F. Neumark, Appl. Phys. Lett. **85**, 3833 (2004).
[4]M. M. Arafat, B. Dinan, S. A. Akbar, and A. S. M. A. Haseeb, Sensors **12**, 7207 (2012).
[5]L. Luo, Y. Zhang, S. S. Mao, and L. Lin, Sens. Actuators, A **127**, 201 (2006).
[6]J. A. Anta, E. Guillen, and R. T. Zaera, J. Phys. Chem. C **116**, 11413 (2012).
[7]M. Willander, O. Nur, Q. X. Zhao, L. L. Yang, M. Lorenz, B. Q. Cao, J. Z. Perez, C. Czekalla, G. Zimmermann, M. Grundmann, A. Bakin, A. Behrends, M. Al-Suleiman, A. El-Shaer, A. C. Mofor, B. Postels, A. Waag, N. Boukos, A. Travlos, H. S. Kwack, J. Guinard, and D. L. S. Dang, Nanotechnology **20**, 332001 (2009).
[8]Y. Yang, X. W. Sun, B. K. Tay, G. F. You, S. T. Tan, and K. L. Teo, Appl. Phys. Lett. **93**, 253107 (2008).
[9]D. C. Look, C. Coskun, B. Claflin, and G. C. Farlow, Physica B **340–342**, 32 (2003).
[10]J. B. You, X. W. Zhang, S. G. Zhang, H. R. Tan, J. Ying, Z. G. Yin, Q. S. Zhu, and P. K. Chu, J. Appl. Phys. **107**, 083701 (2010).
[11]Dhananjay, J. Nagaraju, and S. B. Krupanidhi, Mater. Sci. Eng., B **137**, 126 (2007).
[12]M. Dutta and D. Basak, Appl. Phys. Lett. **92**, 212112 (2008).
[13]G. Z. Jia, B. X. Hao, X. C. Lu, X. L. Wang, Y. M. Li, and J. H. Yao, Acta Phys. Pol., A **124**, 74 (2013).
[14]H. K. Lee, M. S. Kim, and J. S. Yu, Nanotechnology **22**, 445602 (2011).
[15]S. Al-Heniti, R. I. Badran, A. Umar, A. Al-Ghamdi, S. H. Kim, F. Al-Marzouki, A. Al-Hajry, S. A. Al-Sayari, and T. Al-Harbi, J. Nanosci. Nanotechnol. **11**, 1 (2011).
[16]S. Chirakkara and S. B. Krupanidhi, Thin Solid Films **520**, 5894 (2012).
[17]S. Aksoy and Y. Caglar, Superlattices Microstruct. **51**, 613 (2012).
[18]J. H. Werner and H. H. Guttler, J. Appl. Phys. **69**, 1522 (1991).
[19]R. T. Tung, Phys. Rev. B **45**, 13509 (1992).
[20]S. Yılmaz, E. Bacaksız, I. Polat, and Y. Atasoy, Curr. Appl. Phys. **12**, 1326 (2012).
[21]D. Somvanshi and S. Jit, IEEE Trans. Nanotechnol. **13**, 62 (2014).
[22]R. Singh, M. Kumar, and S. Chandra, J. Mater. Sci. **42**, 4675 (2007).
[23]A. E. Morales, E. S. Mora, and U. Pal, Rev. Mexi. Def. S **53**, 18 (2007).
[24]K. Senthil, Y. Tak, M. Seol, and K. Yong, Nano. Res. Lett. **4**, 1329 (2009).
[25]C. Y. Kung, S. L. Young, H. Z. Chen, M. C. Kao, L. Horng, Y. T. Shih, C. C. Lin, T. T. Lin, and C. J. Ou, Nano. Res. Lett. **7**, 372 (2012).
[26]A. Umar, B. Karunagaran, E. K. Suh, and Y. B. Hahn, Nanotechnology **17**, 4072 (2006).
[27]R. Ghosh and D. Basak, Appl. Phys. Lett. **90**, 243106 (2007).
[28]V. Quemener, M. Alnes, L. Vines, P. Rauwel, O. Nilsen, H. Fjellvag, E. V. Monakhov, and B. G. Svensson, J. Phys. D: Appl. Phys. **45**, 315101 (2012).
[29]D. Somvanshi and S. Jit, IEEE Electron Device Lett. **34**, 1238 (2013).
[30]S. Karatas, S. Altindal, A. Turut, and A. Ozmen, Appl. Surf. Sci. **217**, 250 (2003).
[31]H. Asil, K. Cinar, E. Gur, C. Coskun, and S. Tuzemen, Int. J. Phys. Sci. **8**, 371 (2013).
[32]E. Arslan, S. Altindal, S. Ozcelik, and E. Ozbay, Semicond. Sci. Technol. **24**, 075003 (2009).

[This article is copyrighted as indicated in the article. Reuse of AIP content is subject to the terms at: http://scitation.aip.org/termsconditions. Downloaded to ] IP: 136.165.238.131 On: Wed, 24 Dec 2014 00:28:00